

Surface profile measurement using spatially dispersed short coherence interferometry

This content has been downloaded from IOPscience. Please scroll down to see the full text.

2014 Surf. Topogr.: Metrol. Prop. 2 024001

(<http://iopscience.iop.org/2051-672X/2/2/024001>)

View [the table of contents for this issue](#), or go to the [journal homepage](#) for more

Download details:

IP Address: 161.112.232.221

This content was downloaded on 23/05/2014 at 15:26

Please note that [terms and conditions apply](#).

Surface profile measurement using spatially dispersed short coherence interferometry

Mothana A Hassan, Haydn Martin and Xiangqian Jiang

Centre for Precision Technologies, University of Huddersfield, Huddersfield HD1 3DH, UK

E-mail: x.jiang@hud.ac.uk

Received 9 August 2013

Accepted for publication 21 October 2013

Published 23 January 2014

Abstract

Improved online techniques for surface profile measurement can be beneficial in high/ultra-precision manufacturing, in terms of enabling manufacture and reducing costs. This paper introduces a spatially dispersed short-coherence interferometer sourced by a super luminescent diode. This technique uses a broadband light source, which is spatially dispersed across a surface using a reflective grating and a scan lens. In this way, the phase data pertaining to surface at height is spectrally encoded. The light reflected from the surface is interfered with a reference beam in a Michelson interferometer, after which the resulting fringes are interrogated by a spectrometer. Phase shifting interferometry is used to extract the spectrally encoded phase information by analysing four captured frames using a Carré algorithm procedure; in this way, surface height can be determined across a profile on a sample. The short coherent light utilized in this interferometric technique means it has the potential for an application as a remote probe through an optical fibre link. This paper describes the concept of a spatially dispersed short coherence interferometer and provides some of the initial experimental results.

Keywords: optical metrology, surface measurement, interferometry, phase shifting

Nomenclature

SLD	super luminescent diode
SWLI	scanning white light interferometry
OPD	optical path difference
PSI	phase shifting interferometry
PZT	piezo-electric transducer
BS	beam splitter
PC	personal computer
DAQ	data acquisition

1. Introduction

Optical interferometry has been widely explored for surface measurement as a non-contact method. Interferometric methods have many advantages when compared to traditional contact stylus instruments. They do not make any mechanical contact with the surface being measured and thus cannot cause damage under normal circumstances [1–3]. Non-contact methods are generally faster and remain

capable of high-precision measurement. In the field of surface metrology, there are many types of developed techniques including scanning white light interferometry (SWLI), phase shifting interferometry (PSI) and wavelength scanning interferometry [4]. SWLI in particular is a powerful technique, which can overcome the inherent phase ambiguity and is thus capable of measuring discontinuous surface features. As such, SWLI is the *de facto* optical profilometry technique in industrial use. However, for many dynamic applications, such as the analysis of defects on moving substrates, methods such as SWLI are not suitable due to the requirements of mechanically moving the objective lens in order to make the measurement. For applications such as defect detection in roll-to-roll manufacture, it is often enough to have to measure only a line profile on the surface because the second lateral axis of the measurement is provided for by the movement of the substrate.

In this paper, we introduce a spectrally resolved broadband interferometry technique to measure surface profiles at the nanoscale. A Michelson interferometer is setup and illuminated with a broadband super luminescent



diode (SLD) light source. The light is spatially dispersed across a profile on the measurand using a grating and collimating lens. The resulting broadband interferogram is spectrally decomposed and the optical phase is determined for each sampled wavelength simultaneously. This spectrally resolved phase information can be used for interferometric measurement of surface topography by virtue of its relationship to the optical path length in the interferometer [5].

The spatially dispersed interferometer gives surface topography information across a profile on a measurand. The length and sampling resolution of this profile depend on the numerical aperture and aberration properties of the objective lens, as well as the properties of the grating and the specification of the spectrometer [6, 7].

2. Principle of operation

PSI is widely used in interferometry utilizing monochromatic light sources. The limitation of the method is an inherent phase ambiguity because of the inability to determine the absolute fringe order. This means a limitation for this technique when used for surface profiling, in which the wavefront is reflected from the measurand surface; the height difference between two sampled points should not exceed one quarter of the source wavelength. However, increases in height of greater than this limit may be tracked by using a phase unwrapping process as long as the maximum discontinuous height change condition is met by neighbouring points across the whole measurement [8].

In this section, the principle of a spatially dispersed broadband PSI technique is explained. The experimental apparatus is based upon a Michelson interferometer configuration. The measurement arm is formed from a dispersive probe and the surface under test. The reference arm comprises a mirror mounted on a piezo-electric transducer (PZT) to act as the phase shifting element. Without considering temporal coherence, which depends on the source and is a function of OPD, the resultant intensity of the interfered beam from an interferometer can be described as

$$I = I_r + I_m + 2\sqrt{I_r I_m} \cos(\phi), \quad (1)$$

where I_r and I_m are the irradiance reflected from the reference mirror and the surface under test respectively. ϕ is the phase difference between them as the path lengths which is related to the surface topography.

The PSI method can be used to analyse collected intensity data to determine the phase. The intensity pattern is recorded as the path length in the reference arm is changed sequentially. The recorded interferograms are analysed and a suitable algorithm recovers the phase. Examples of these algorithms are Carré, Schwider–Hariharan and three step, although many more have been developed [9, 10]. The Carré algorithm is potentially the most useful for the experimental apparatus in this work, because it does not require a specific value of phase shift, it only requires each shift to be identical, which has benefits for a system operating at multiple wavelengths, where the same physical movement of the optical path length results

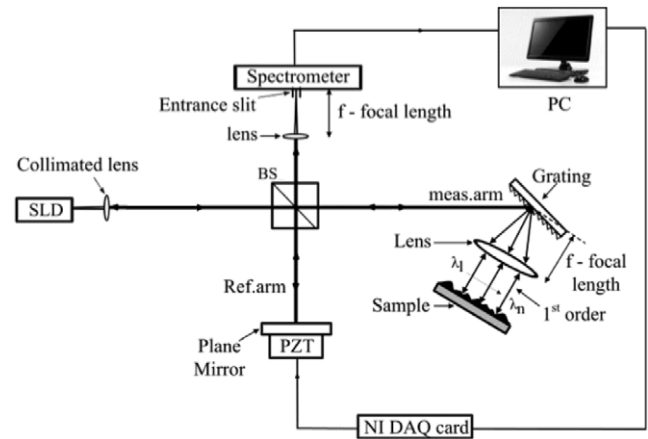


Figure 1. Experimental setup.

in a phase shift that varies with the wavelength. The Carré algorithm is given as

$$\phi = \tan^{-1} \left\{ \frac{[3(I_2 - I_3) - (I_1 - I_4)][(I_1 - I_4) + (I_2 - I_3)]^{1/2}}{(I_2 + I_3) - (I_1 + I_4)} \right\}. \quad (2)$$

Four phase-shifted measurement intensities: I_1 , I_2 , I_3 and I_4 are required in order to extract the original phase. In our apparatus, each wavelength, λ which is discretized through analysis by the CCD spectrometer, is mapped by the dispersive optical probe to a single position, x along a line profile on the surface under test. The phase of the interference fringes at any given wavelength is then a function of the optical path difference (OPD) and thus the surface height, h at the position, x . This may be represented as

$$I(x, \lambda) = I_r(\lambda) + I_m(x_\lambda) + 2\sqrt{I_r(\lambda) I_m(x_\lambda)} \cos \phi(x, \lambda), \quad (3)$$

where

$$\phi(x, \lambda) = \frac{4\pi}{\lambda} h_x. \quad (4)$$

Note that there is no x dependence in the reference arm intensity because it contains only a simple mirror. From equation (4), the surface height can be calculated for any continuous phase distribution. The phase difference between the reflected wave surface under test and the reference wave can be calculated by evaluating the fringe intensity. The interferogram is position encoded by the wavelength along the profile, x . By determining the phase difference at a given wavelength, the surface height of the corresponding position may be determined.

3. Experimental setup

The basic configuration of the surface measurement apparatus is illustrated in figure 1.

The experimental setup is a PSI comprising a Michelson interferometer, which features: a grating element and collimating lens in the measurement arm to produce a dispersive probe; a spectrometer to analyse the spectral

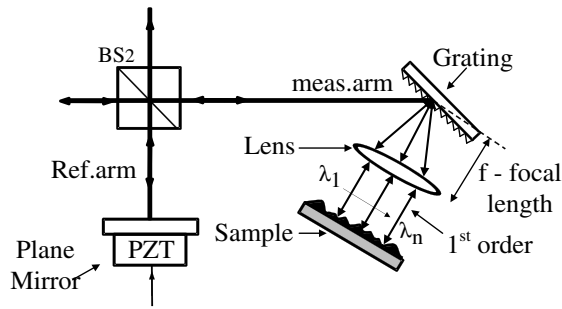


Figure 2. Optical probing and reference arm.

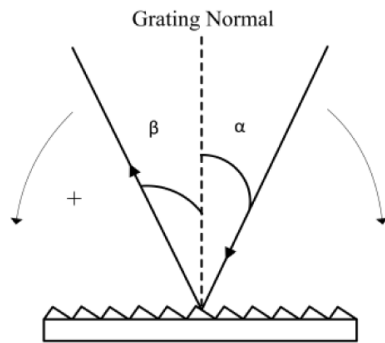


Figure 3. Utilized angle and sign convention.

interferogram generated; and a PZT in the reference arm to shift the reference phase. A SLD (Exalos EXS8310–8411) is used as a broadband light source and features high spatial coherence while maintaining a short coherence length of approximately 20–30 μm . The SLD has an output power of 1.08 mW, at a bandwidth of 25 nm (full-width at half-maximum) centred at 825 nm. The beam splitter acts as the main splitter/combiner for the Michelson interferometer. The measurement arm beam propagates through the dispersive probe to the sample; the reference beam is incident on the PZT mounted mirror (see figure 2). In the dispersive optical probe, the SLD beam is angularly dispersed by the grating. The dispersed light is then collimated and then focused as a line profile onto the sample. In the dispersive optical probe, the broadband SLD beam (width 8.3 mm) is angularly dispersed by the grating. The dispersed light is then collimated and focused onto the surface by the objective lens. The lens used for this experiment was an achromatic doublet (Thorlabs, AC254–050-B) with a focal length of 50 mm. The grating equation is

$$m\lambda = d(\sin \alpha + \sin \beta), \quad (5)$$

where m is an integer number, d is the grating pitch and λ is the wavelength of the incident light. α , β are the incident and diffracted angles respectively, as shown in figure 3.

The first-order diffracted beam is used to probe the surface being tested using the objective lens. The lateral range (line profile length), S , of the incident light on the surface can be represented by

$$S = f \frac{\Delta\lambda}{d \cos \beta}, \quad (6)$$

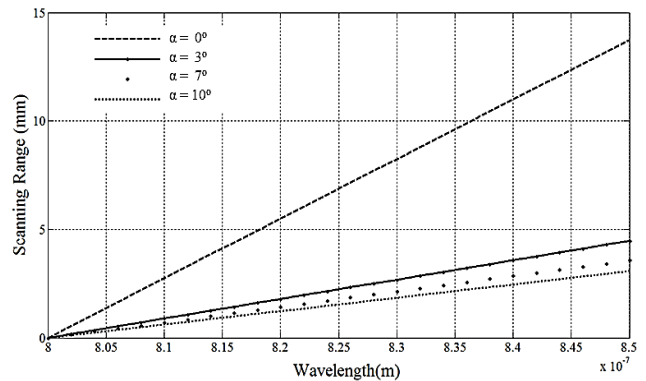


Figure 4. Scan linearity versus various angles of incidence.

where f is the effective focal length of the objective lens and the diffraction grating is operating on the first order only. The rear focal point of the objective lens is aligned such that it is placed at the point of diffraction on the grating surface. The optical axis of the lens is aligned with the axis of propagation of the centre SLD wavelength (825 nm). The grating is set so that the incident angle of the measurement arm beam is 0° , which results in a diffracted angle of 83.70° at the centre wavelength and an angular dispersion of 0.01 rad nm^{-1} . The incident angle is critical in determining the angular dispersion and thus the overall length of the line profile cast upon the surface. Figure 4 shows the calculated scan ranges for several different incident angles. It is evident from the figure that the smaller the incident angle, the larger the scan range. In addition, it was found that the scan range is, to a good approximation, linear across the wavelength scan range. The first order diffracted beam from the grating is collimated and focused by the objective lens onto the surface being tested. In the reference arm, a PZT (Physik Instrumente, P.810.10) mounted mirror is used to generate the phase by moving the mirror through four positions along the optical axis. The spectral interferogram is recorded by a spectrometer (Solar Laser Systems, S150) after each mirror movement to provide the set of intensities required for applying the Carré PSI algorithm. The spectrometer features a CMOS line array with 3648 pixels and has a specified wavelength resolution of 0.06 nm. The PSI operation is coordinated using National Instruments Labview software and a data acquisition (DAQ) card having an analogue output (National Instruments USB-6211). In the reference arm, the PZT is pushed in four steps by applying a series of 0.84 V steps using the analogue output on the DAQ card.

4. Experimental results and discussion

In the described experimental work, the spectral interferogram generated from the wavefronts reflected from the test surface and the reference mirror were analysed using the spectrometer. A spectrogram was captured for each of the four reference mirror positions, relating to induced phase shifts of approximately 110° at the source centre wavelength of 825 nm. The reference mirror is moved in 1 s intervals with the spectrogram data being read after a delay of 2 ms,

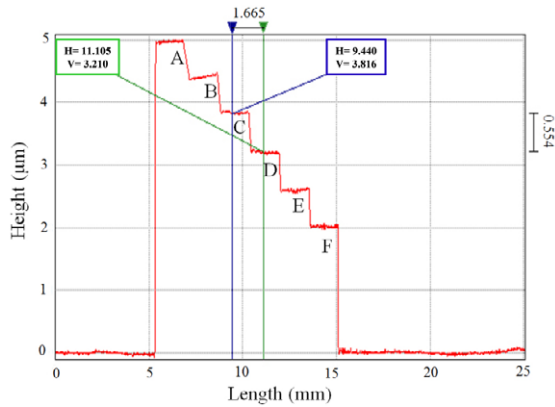


Figure 5. Surfstand analysis of the multi-step artefact measured with the Taylor Hobson PGI.

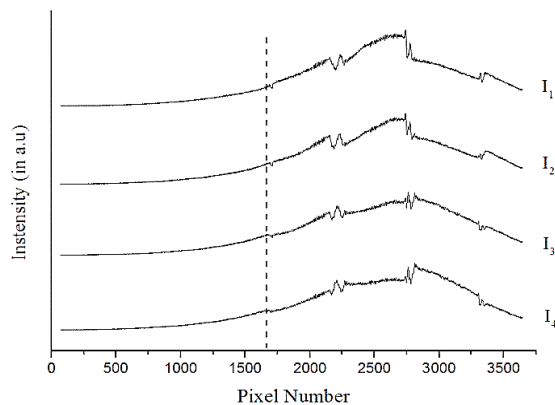


Figure 6. Spectral interferograms captured with four mirror shifts.

to allow for mechanical settling. In combination with the dispersive optical probe, each pixel of the spectrometer monitors interferogram intensity information retrieved from one specific position in the surface. The spectral interferogram data is transferred to the personal computer (PC) through a USB interface and analysed using National Instruments Labview software. In this paper, a diamond turned multi-step artefact, having variable slope angles between steps, was used to investigate the measurement concept. Figure 5 shows a surface profile of this sample obtained using a Taylor Hobson PGI stylus instrument and the University of Huddersfield's proprietary surface analysis software, Surfstand.

In the experimental setup, the optical probe was arranged such that the four left-most steps (A, B, C and D in figure 5) were imaged. Figure 6 shows the retrieved spectral interferograms at the four reference mirror positions using the multi-step artefact. The position corresponding to the start of step A (figure 5) is located approximately at spectrometer pixel number 1700. The curvature of the intensity profile is directly due to the optical power spectrum of the SLD source used in the experiment. The data from the four acquired interferograms were then evaluated by the Carré phase shifting algorithm in order to extract the phase information relating to the surface height distribution along the profile. The raw extracted phase profile is shown in figure 7. The raw phase dataset was then unwrapped by tracking any phase changes

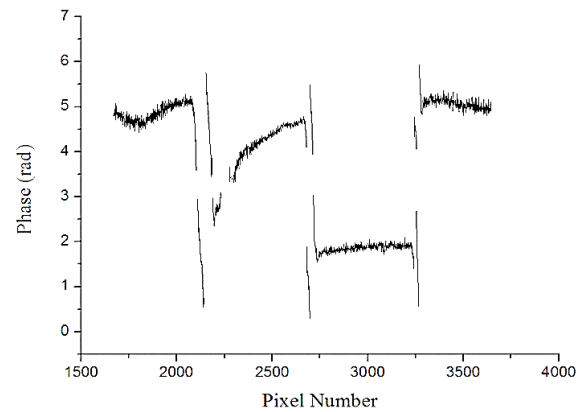


Figure 7. Raw phase profile calculated with the Carré algorithm.

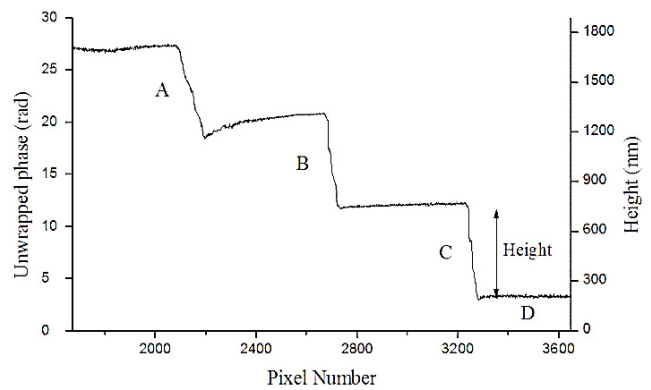


Figure 8. Unwrapped phase profile.

of more than π and adjusting the fringe order up or down as necessary. The result of this process, showing the properly extracted phase profile, is shown in figure 8. It is worthy of note that the step heights for the multistep sample are actually larger than the non-ambiguous measurement range of approximately 206 nm ($\lambda/4$). However, because the steps are joined with angled slopes rather than by a sharp transition, it is possible for the apparatus to track the transition with the currently implemented objective lens. The phase profile in figure 8 was converted to a surface height profile using equation (4).

Comparing the profile extracted using the Taylor Hobson PGI stylus profilometer (figure 5) to that obtained using the spatially dispersed short coherence method, it is clear that the step heights have been successfully resolved. The step profile seen in figure 8 is a subset of the steps referred to as A, B, C and D in figure 5. It is evident on comparison of the two results that there is some distortion apparent on the left hand side of figure 8. This is likely to be due to a combination of imperfect alignment in the optical probe apparatus and inherent aberrations in the simple single lens objective. These issues can be alleviated with better alignment and calibration of the probe against an optical flat. Steps C and D appear to be well resolved and as such were used to confirm the validity of the method by gauging the step height. A mean line was taken from the data in the middle portions of each step and the difference between them calculated.

The calculated step height between steps C and D was 543.66 nm compared to the Surfstand/PGI result (figure 5) of 554 nm. This result confirms the validity of the method; we consider that further investigation into a more optimized optical probe configuration, as well as the development of a suitable calibration routine, will reduce any discrepancy further.

5. Conclusion

In this paper a spatially dispersed short coherence surface profiling interferometry technique was used to obtain the surface profile of a multi-step sample. The method combines a SLD light source with an optical probe that spatially disperses the source light across a profile on a surface. An interferogram is generated, which is then analysed spectrally. Each wavelength component of the spectral interferogram corresponds to a specific lateral position along the surface profile. The Carré phase shifting algorithm was used to extract the phase information and thus determine a surface height profile, from multiple phase shifted interferograms. The step heights were found to be in approximate agreement with those calculated from a Taylor Hobson PGI stylus profilometer although there was evidence of some distortion, likely due to a combination of non-optimal optical alignment and inherent aberration in the simple lens system used. This will be improved in future work with better probe design and the introduction of a calibration routine using an optical flat. Other future improvements to this proof of concept structure will be the investigation of faster phase analysis methods e.g. Fourier transform profilometry, to improve stability of measurement under environmental perturbation and make the system more applicable to dynamic measurement applications involving moving substrates. Higher NA probes also need to be investigated to increase lateral resolution.

This reported technique is based on short coherence light and as such it has the potential for an application with a fibre linked probe. The reference and measurement waves may travel through the same fibre if they are separated by an optical path difference much greater than the coherence length of the SLD (a few tens of microns). In this way, both waves experience common fibre induced disturbances, thus circumventing the instabilities usually associated with

fibre interferometers. Such a probe could have uses for submicron defect detection in moving substrates in roll-to-roll manufacturing processes, for instance.

Acknowledgments

The authors gratefully acknowledge the UK's Engineering and Physical Sciences Research Council (EPSRC) funding of the EPSRC Centre for Innovative Manufacturing in Advanced Metrology (Grant Ref: EP/I033424/1), the European Research Council funding by the SURFUND Advanced Grant (228117) as well as a studentship funded by the Department of Laser and Optoelectronics Engineering at the University of Technology, Iraq.

References

- [1] Lonardo P M, Lucca D A and de Chiffre L E 2002 Emerging trends in surface metrology *Ann. CIRP* **51** 701–23
- [2] Dhanasekar B, Mohan N, Bhaduri B and Ramamoorthy B 2008 Evaluation of surface roughness based monochromatic speckle correlation using image processing *Precis. Eng.* **32** 196–206
- [3] De Chiffre L, Kunzmann H, Peggs G N and Lucca D A 2003 Surfaces in precision engineering, micro-engineering and nanotechnology *Ann. CIRP* **52** 561–77
- [4] Jiang X *et al* 2010 Fast surface measurement using wavelength scanning interferometry with compensation of environmental noise *Appl. Opt.* **49** 2903–9
- [5] Sainzy C, Calatroni J E and Tribillon G 1990 Refractometry of liquid samples with spectrally resolved white light interferometry *Meas. Sci. Technol.* **1** 356–61
- [6] Sandoz P, Tribillon G and Perrin H 1996 High resolution profilometry by using phase calculation algorithms for spectroscopic analysis of white light interferograms *J. Mod. Opt.* **43** 701–8
- [7] Calatroni A L, Guerrero, Sainz C and Escalona R 1996 Spectrally-resolved white-light interferometry as a profilometry tool *Opt. Laser Technol.* **28** 485–9
- [8] Caber P J 1993 Interferometric profile for rough surfaces *Appl. Opt.* **32** 3438–41
- [9] Carré P 1966 Installation et utilisation du comparateur photoélectrique et interférentiel du Bureau International des Poids et Mesures *Metrologia* **2** 13–23
- [10] Schreiber H and Bruning J H 2007 *Optical Shop Testing* 3rd edn, ed D Malacara (Hoboken, NJ: Wiley) pp 547–666